ARTICLE

WILEY **BIOTECHNOLOGY** **BIOENGINEERING**

High-throughput combinatorial screening reveals interactions between signaling molecules that regulate adult neural stem cell fate

Riya Muckom[1] | Sean McFarland[2] | Chun Yang[1] | Brian Perea[1] | Megan Gentes[1] | Abirami Murugappan[1] | Eric Tran[1] | Jonathan S. Dordick[3] | Douglas S. Clark[1] | David V. Schaffer[1,2]

[1]Department of Chemical and Biomolecular Engineering, University of California, Berkeley, California

[2]Department of Bioengineering, University of California, Berkeley, California

[3]Department of Chemical and Biological Engineering, Rensselaer Polytechnic Institute, Troy, New York

Correspondence
Douglas S. Clark, Department of Chemical and Biomolecular Engineering, University of California, 497 Tan Hall, Berkeley 94720-3220, CA.
Email: dsc@berkeley.edu;
David V. Schaffer, Department of Bioengineering, University of California, 278 Stanley Hall, Berkeley 94720-3220, CA.
Email: schaffer@berkeley.edu

Abstract

Advancing our knowledge of how neural stem cell (NSC) behavior in the adult hippocampus is regulated has implications for elucidating basic mechanisms of learning and memory as well as for neurodegenerative disease therapy. To date, numerous biochemical cues from the endogenous hippocampal NSC niche have been identified as modulators of NSC quiescence, proliferation, and differentiation; however, the complex repertoire of signaling factors within stem cell niches raises the question of how cues act in combination with one another to influence NSC physiology. To help overcome experimental bottlenecks in studying this question, we adapted a high-throughput microculture system, with over 500 distinct microenvironments, to conduct a systematic combinatorial screen of key signaling cues and collect high-content phenotype data on endpoint NSC populations. This novel application of the platform consumed only 0.2% of reagent volumes used in conventional 96-well plates, and resulted in the discovery of numerous statistically significant interactions among key endogenous signals. Antagonistic relationships between fibroblast growth factor 2, transforming growth factor β (TGF-β), and Wnt-3a were found to impact NSC proliferation and differentiation, whereas a synergistic relationship between Wnt-3a and Ephrin-B2 on neuronal differentiation and maturation was found. Furthermore, TGF-β and bone morphogenetic protein 4 combined with Wnt-3a and Ephrin-B2 resulted in a coordinated effect on neuronal differentiation and maturation. Overall, this study offers candidates for further elucidation of significant mechanisms guiding NSC fate choice and contributes strategies for enhancing control over stem cell-based therapies for neurodegenerative diseases.

KEYWORDS
combinatorial, high-throughput, hippocampus, niche, NSC

1 | INTRODUCTION

Stem cells, defined as immature cells capable of self-renewal and differentiation into a range of mature cell types, play fundamental roles in tissue formation and maintenance, and have broad applications for in vitro disease modeling, drug screening, and in vivo tissue regeneration (Avior, Sagi, & Benvenisty, 2016; Lader, Stachel, & Bu, 2017; Pelttari, Mumme, Barbero, & Martin, 2017; Rodrigues, Gomes, & Reis, 2011; Rossi & Keirstead, 2009). Neural stem cells (NSCs) in the hippocampus of the adult brain are of particular interest because of their potential to proliferate and differentiate into new neurons and glia throughout adulthood (Gage, Kempermann, Palmer, Peterson, & Ray, 1998). These tightly regulated NSC processes have impact on learning and memory, as well as implications for the treatment of neurodegenerative disorders such as Alzheimer's disease (Gonçalves, Schafer, & Gage, 2016).

Adult hippocampal NSCs reside within the dentate gyrus of the subgranular zone—a complex and intricate niche that presents various forms of instructive regulatory stimuli. Numerous studies have identified a range of individual endogenous signaling molecules that regulate NSC quiescence, proliferation, and/or differentiation. For example, early studies on primary NSCs isolated from the adult rodent hippocampus established a proliferative effect of fibroblast growth factor 2 (FGF-2; Palmer, 1995; Palmer, Markakis, Willhoite, Safar, & Gage, 1999) and sonic hedgehog (SHH) was subsequently found to promote proliferation in vitro and in vivo (Lai, Kaspar, Gage, & Schaffer, 2003; Lai, Robertson, & Schaffer, 2004). Furthermore, Wnt-3a and Ephrin-B2 ligands within the NSC niche were discovered to regulate neurogenesis (Ashton et al., 2012; Lie et al., 2005), whereas bone morphogenetic protein 4 (BMP-4) and most recently transforming growth factor β (TGF-β) signals have been associated with quiescence of adult hippocampal NSCs (Bond et al., 2014; Kandasamy et al., 2014; Mira et al., 2010; Yousef et al., 2014, 2015).

While such reductionist studies have greatly advanced our knowledge of NSC regulators, these cells are likely exposed to multiple cues simultaneously within the niche (Supporting Information Figure S1; Lein et al., 2007) and the potential effects of their combinatorial presentation within the hippocampal NSC niche have not yet been examined. Unfortunately, experimental capabilities to examine such interactions using conventional well-plate platforms are constrained by reagent costs and feasibility as the parameter space for unbiased and systematic combinatorial studies grows exponentially, for example, 2^n possible combinations can be formed from n different factors.

To overcome these limitations, many researchers have adopted novel miniaturized cell culture platforms for dissecting analogous cell niches, (Brafman et al., 2009; Flaim, Teng, Chien, & Bhatia, 2008; Gobaa et al., 2011; LaBarge et al., 2009; Rasi Ghaemi et al., 2016; Roccio et al., 2012; Soen, Mori, Palmer, & Brown, 2006) and in some cases these studies have revealed nonintuitive cell behavior that would be difficult to detect without an unbiased screen (Titmarsh et al., 2016; Wang et al., 2016). Accordingly, here we have adapted and demonstrated the utility of a high-throughput microculture platform (Figure 1a), previously applied toward toxicological assays (Kwon et al., 2014; Lee et al., 2014; Nierode et al., 2016) enabling independent preparation and control of media and cell substrates, simultaneous media replenishment of over 500 microcultures, and higher exposure to microcultures for immunocytochemistry. After platform optimization and characterization, we used a full factorial design to systematically expose NSCs to combinatorial niche signals and collected high-content image data (Boutros, Heigwer, & Laufer, 2015) of NSC proliferation, neuronal/glial differentiation, and morphology (Figure 1b,c). We discovered that antagonistic relationships among FGF-2, TGF-β, and Wnt-3a impact NSC proliferation and differentiation, and that a synergistic relationship between Wnt-3a and Ephrin-B2 promotes neuronal differentiation and maturation. Furthermore, we observed that TGF-β and BMP-4 in combination with Wnt-3a and Ephrin-B2 exhibited a coordinated effect on neuronal differentiation and maturation. Finally, we arranged conditions based on similarity in the direction and extent of phenotypic responses to identify broader trends across combinatorial signaling environments.

2 | EXPERIMENTAL PROCEDURES

2.1 | Primary adult hippocampal NSC culture

Adult rodent NSCs were cultures as described previously (Peltier et al., 2010). NSCs were subcultured in Dulbecco's modified Eagle's medium-F12 + N_2 supplement and 20 ng/ml FGF-2 on laminin-coated polystyrene dishes. NSCs were dissociated with Accutase (Sigma-Aldrich, St. Louis, MO) for replating upon confluency and seeding into conventional plate and microculture experiments.

2.2 | Synthesis of multivalent ephrin-B2

An Ephrin type-B receptor 4 (EphB4) binding peptide TNYLFSPNG-PIARAW (Koolpe, Burgess, Dail, & Pasquale, 2005), with K_D = 70 nM, previously identified by phage display was conjugated to a 1,500-kDa hyaluronic acid (HA) chain to generate a multivalent ligand. A bifunctional molecule N-ε-maleimidocaproic acid hydrazide was utilized to bridge HA and the peptide of interest, where it was first reacted with the carboxylic acid functional group on HA to generate an amide, and subsequently reacted with the thiol group on the EphB4 binding peptide. The valency of the multivalent peptide conjugate is 40, which was calculated as the molar ratios of HA to ligand, as determined by the bicinchoninic acid assay assay, a method that was previously confirmed by size exclusion chromatography coupled with multiangle static light scattering measurement (Conway et al., 2013).

2.3 | NSC microculture on pillar/well chip system

Micropillar and microwell chips (MBD, Gyeonggi-do, Korea) made of polystyrene were manufactured by plastic injection molding as described previously (Kwon et al., 2014; Lee et al., 2014). The micropillar culture chip was coated in laminin by placing into a
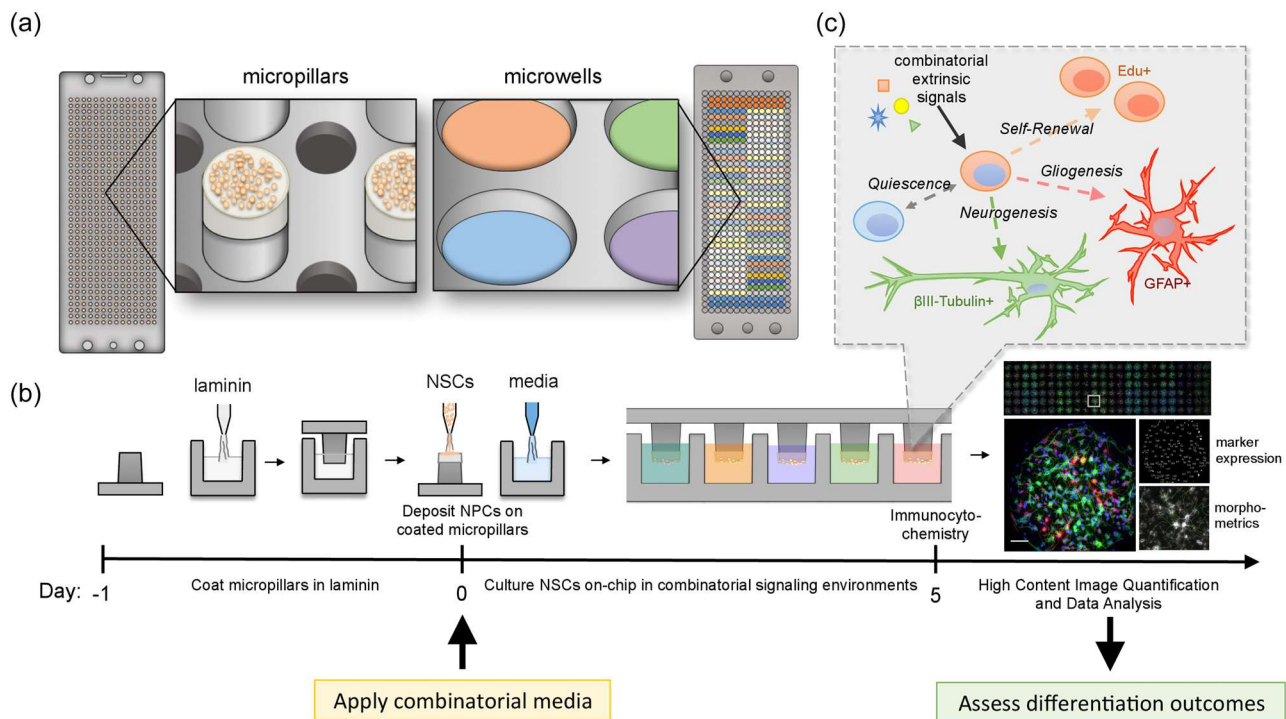
FIGURE 1 High-throughput micropillar and microwell culture system for high-content screening of stem cell proliferation and differentiation. (a) The high-throughput cell culture array consists of complementary micropillars and microwells that combine to form 532 independent cell culture environments; micropillars have a diameter of 750 μm and are spaced 1 mm apart, and microwells contain up to 800 nl of media. (b) Timeline of an immunocytochemistry assay to quantify NSC proliferation and differentiation. NSCs in a 60-nl suspension were deposited on the surface of the laminin-coated micropillars to form a monolayer culture, and cell culture media containing select chemical signaling cues were robotically dispensed into the corresponding microwells. Micropillars were inverted into the microwells, and media was replenished every other day until the endpoint. (c) NSCs were exposed to systematic combinations of soluble cues to recapitulate the complexity of the in vivo hippocampal niche where combinatorial extrinsic signals guide phenotypic processes including self-renewal, gliogenesis, neurogenesis, quiescence, and death. GFAP: glial fibrillary acidic protein; NSC: neural stem cell [Color figure can be viewed at wileyonlinelibrary.com]

microwell chip (MBD) containing a solution of laminin diluted in sterile phosphate-buffered saline (PBS) overnight. NSCs in suspension were deposited onto the laminin-coated micropillar and left pillar side up for at least 30 min to allow NSCs to settle and adhere to the surface. The micropillar chip was then inverted and placed into a fresh microwell chip containing cell culture media. All liquid dispensing into the microculture platform was performed with a DIGILAB Omnigrid Micro (DIGILAB, Hopkinton, MA) liquid handler with customized programs for deposition patterns. Media was changed daily by transferring the micropillar chip into a microwell chip containing fresh media every other day using a custom-made mechanical "Chip Swapper" (R. Muckom, Berkeley, CA) for consistent transfer. Technical replicates included two different dispensing patterns to average out positional effects across the microchip.

2.4 | On-chip viability assay

At the endpoint of the experiment, the micropillar chip was carefully removed from the well chip and placed in new well chip containing calcein AM, ethidium homodimer, and Hoechst diluted in sterile PBS (dilution details in Supporting Information Table S2). The chip was incubated for 20 min and then transferred to a new well chip

containing PBS, and individual microenvironments were imaged using fluorescent microscopy.

2.5 | On-chip immunofluorescence and proliferation assays

At the endpoint of the experiment, the micropillar chip was carefully removed from the well chip and placed into a bath of 4% parafomaldehyde for 15 min to fix cell cultures. Then, the micropillar chip was washed twice in PBS for 5 min each and placed into a bath of 0.25% Triton-X + 5% donkey serum in PBS for 10 min to permeabilize cells. After permeabilization, the micropillar chip was washed five times in 5% donkey serum for 5 min each, dried, and transferred to a well chip containing primary antibodies of interest diluted in PBS + donkey serum (dilution details in Supporting Information Table S2) and stored overnight at 4°C. After primary staining, the micropillar chip was washed twice in PBS for 5 min each, dried, and then placed into a microwell chip containing the corresponding secondary antibodies (dilution details in Supporting Information Table S2) and incubated at 37°C for 2 hr. After secondary staining, the micropillar chip was washed twice in PBS for 5 min each, dried, and then placed into a well chip containing PBS

and individual microenvironments were imaged using automated wide-field fluorescent microscopy.

2.6 | Well-plate NSC culture and immunocytochemistry

Individual wells in a tissue culture-treated μClear 96-well plate (655090; Greiner Bio-One, Kremsmünster, Austria) were coated with laminin by incubating overnight in a solution of laminin diluted in sterile PBS. On Day 0, NSCs were seeded at a uniform concentration of 2.2E5 cells/ml per well (roughly 40,000 cells/well, or 1.4E3 cells/mm^2). Culture media containing individual and combined signaling cues (dosage details in Supporting Information Table S1) was applied on Day 0 and replaced every other day. On Day 5, cells were fixed in 4% parafomaldehyde for 15 min. Then, cultures were washed twice in PBS for 5 min each and permeabilized in 0.25% Triton-X + 5% donkey serum in PBS for 10 min. After permeabilization, the wells were washed five times in 5% donkey serum for 5 min each and incubated in primary antibodies of interest diluted in PBS + donkey serum (dilution details in Supporting Information Table S2) and stored overnight at 4°C. After primary staining, wells were washed twice in PBS for 5 min each and then incubated in the corresponding secondary antibodies (dilution details in Supporting Information Table S2) at 37°C for 2 hr. After secondary staining, wells were washed twice in PBS for 5 min each. Individual sites within each well were imaged using automated confocal microscopy.

2.7 | Automated wide-field fluorescence microscopy

Stained micropillar chips were sealed with a polypropylene film (T-2452-1; GeneMate, Radnor, PA) and imaged with a 20× objective using a Molecular Devices ImageXpress Micro (Molecular Devices, San Jose, CA) automated wide-field fluorescence microscope available in the Shared Stem Cell Facility at UC Berkeley. Lamp exposure time was kept constant for a fluorescence channel within an imaging set.

2.8 | Automated confocal fluorescence microscopy

Twenty-eight sites within each stained well of a 96-well plate were imaged with a 40× water objective using a Perkin Elmer Opera Phenix automated confocal fluorescence microscope (Perkin Elmer, Waltham, MA) available in the High-Throughput Screening Facility at UC Berkeley. Laser exposure time, gain, and laser power were kept constant for a fluorescence channel.

2.9 | Image processing, data analysis, and statistical methods

Background fluorescence was removed from all images using a rolling bar radius algorithm using ImageJ (NIH, Washington, DC) (Bankhead, 2014). Feature extraction was performed with ImageJ (NIH) application NeuriteTracer (Fournier Lab, Montreal, Quebec, Canada) (Pool, Thiemann, Bar-Or, & Fournier, 2008) and custom image-processing scripts. Quantified image data were then imported into Python for statistical data analysis (Malo, Hanley, Cerquozzi, Pelletier, & Nadon, 2006) and visualization. In brief, raw data were scaled and centered by z-score, and descriptive statistics were calculated from four replicates at the chip-level and six replicates within each chip. Error bars represent 95% confidence intervals unless otherwise specified. A factorial analysis of variance (ANOVA) was used to calculate statistical significance from a group of conditions. Nonsignificant terms were removed to create the ordinary least squares (OLS) model; β parameters were calculated for all significant terms as a simplified measure of their relative contribution to the extent of neurogenesis observed in a population of NSCs. For the hierarchical cluster model, the Euclidean distance was used to measure pairwise distance between each observation and the unweighted pair group method with arithmetic mean algorithm was used to calculate the linkage pattern. Code was available upon request. For validation studies in 96-well plate format, Harmony image analysis software (Perkin Elmer) was used to quantify neurite morphological features. A γ correction of 2.0 was applied to highlight morphological features of select images for clarity in visualization only; quantification of image features was performed with the original images. A Student's t test or Welch's t test was applied to well-averaged data for equal and unequal sample sizes, respectively, with at least n = 3 replicates.

3 | RESULTS

3.1 | Miniaturization and increased throughput of primary NSC culture for phenotypic screening

Our system is composed of two halves—A chip with 532 × 750 μm wide pillars onto which cells can be deposited with a liquid dispensing system and a chip with 532 × 800 nl wells into which culture media and signaling cues can be dispensed, where placing the pillar chip into the well chip enables long-term cell culture and subsequent imaging (Figure 1). NSCs derived from the adult rodent hippocampus are typically propagated in vitro on substrates coated with extracellular matrix protein laminin (Peltier et al., 2010), so initial optimization was performed to identify a coating procedure for laminin that could enable NSC monolayer formation with (a) interpillar consistency and (b) intrapillar uniformity (Supporting Information Figure S2). Subsequently, coating parameters were kept constant for all studies to ensure a consistent and uniform initial condition across all 532 micropillar environments (Figure 2a). Next, we assessed the capacity of the micropillar chip system to maintain NSC viability and reproduce proliferation and differentiation in response to well-characterized cues. A live/dead assay several hours after initial seeding showed a high proportion, >80%, of viable cells across all 532 microenvironments (Figure 2b,c), comparable to seeding into a standard well plate. Additionally, we observed uniform seeding across the entire micropillar chip (Figure 2d) for an even baseline. Next, to assess whether NSC cultures retained the capacities for proliferation and differentiation into neurons and glia, we applied known proliferation-inducing
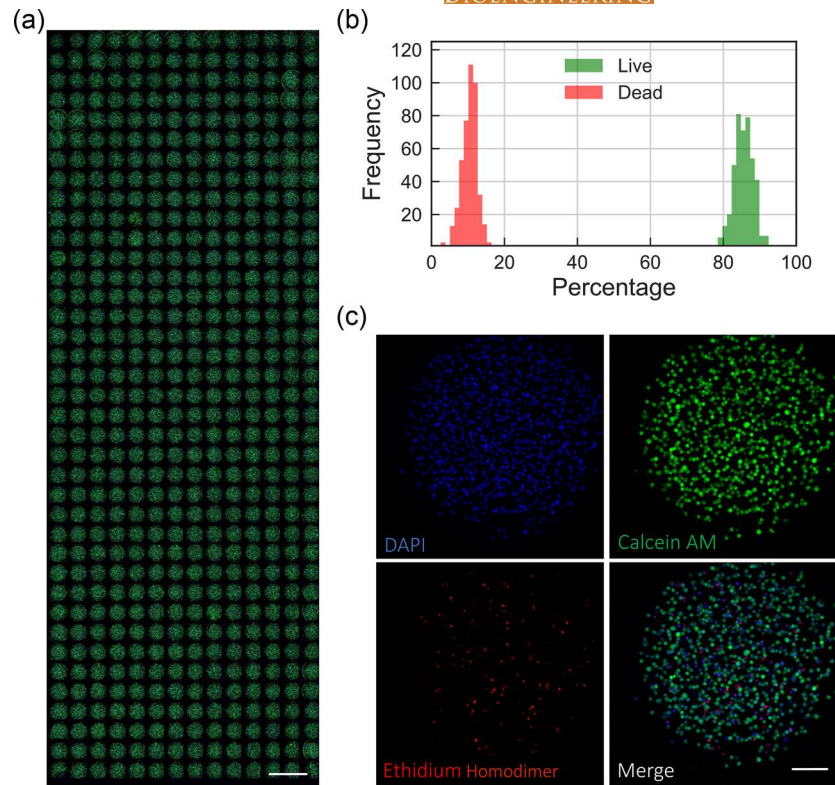
FIGURE 2 Primary NSC cultures on micropillars demonstrated uniform initial seeding and retain viability, proliferation, and differentiation potential. (a) Day 0 montage of NSCs seeded onto 532 microenvironments and stained for calcein AM (green), ethidium homodimer (red), and Hoechst (blue). Scale bar = 2 mm. (b) Histograms of percent live and dead cells across 532 microcultures. (c) The ×20 magnification of stained micropillar culture showing individual fluorescence channels and merge. Scale bar = 100 μm. (d) Quantification of micropillar total cell count by column and by row. (e) Induced proliferation or differentiation on micropillar/microwell culture platform with 20 ng/ml FGF-2 or 1 μM retinoic acid + 1% FBS, respectively. Immunocytochemistry was conducted after 5 days for EdU incorporation or GFAP and β-III-tubulin expression. Scale bar = 100 μm. Error bars represent standard deviation of 24 replicates. AM: acetoxymethyl; DAPI: 4′,6-diamidino-2-phenylindole; FBS: fetal bovine serum; FGF-2: fibroblast growth factor 2; GFAP: glial fibrillary acidic protein; NSC: neural stem cell [Color figure can be viewed at wileyonlinelibrary.com]
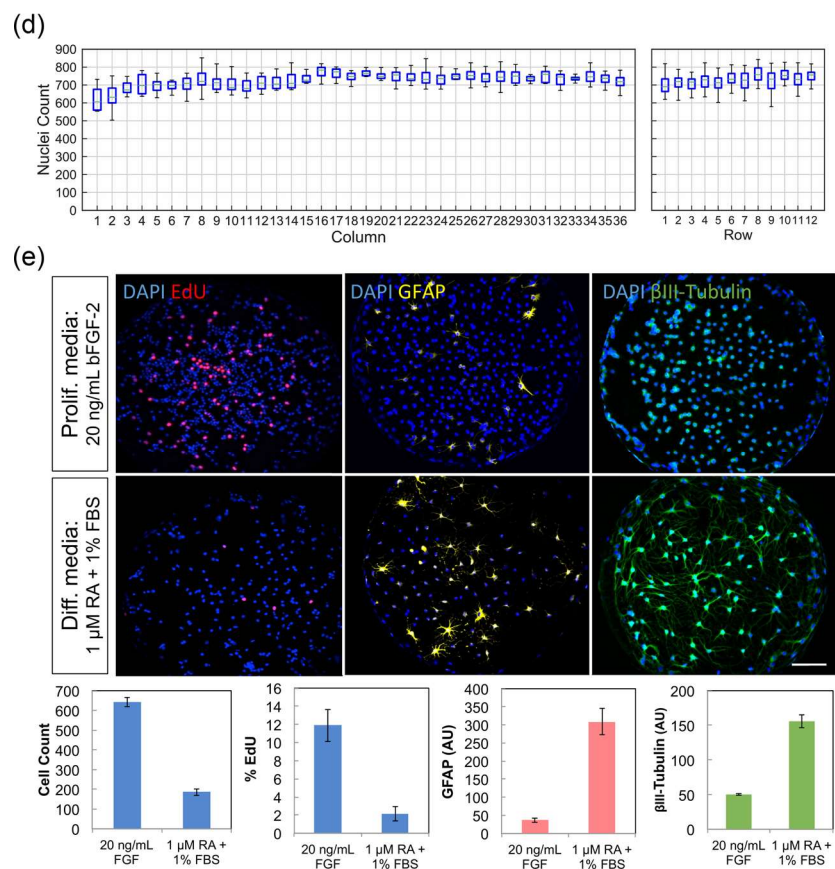
and differentiation-inducing media conditions. Media was replenished by transferring the micropillar chip into a new microwell chip with fresh media every other day. After 5 days, proliferation was measured using an EdU assay, (Invitrogen, Eugene, OR) and differentiation into

neurons and glia was marked with immunocytochemistry of βIII-tubulin and glial fibrillary acidic protein (GFAP), respectively. Anticipated increases in proliferation and differentiation were observed (Figure 2e). Additionally, the Z factors for these and
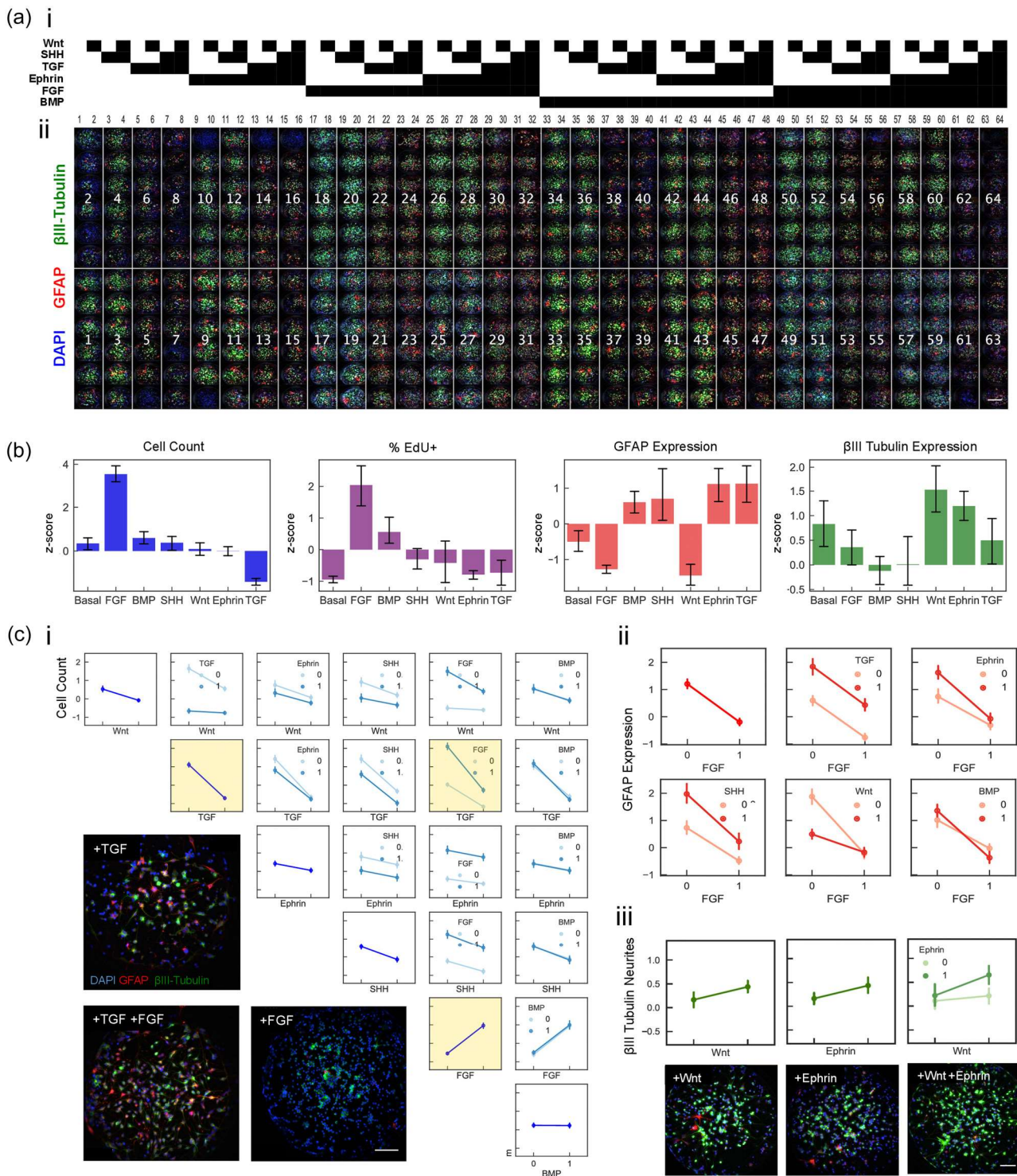
FIGURE 3 Full factorial combinatorial screen of key endogenous signaling cues. (a) i. Design matrix of full factorial experimental conditions involving Wnt-3a, TGF- β, Ephrin-B2, BMP-4, FGF-2, and SHH-N. ii. Montage of immunocytochemistry for 384 microcultures after exposure to full a factorial set of combinations for 5 days. Replicates are grouped within boxes and labeled by condition in i, reagent details and doses are found in Supporting Information Table S1, and staining details are found in Supporting Information Table S2. Scale bar = 500 microns. (b) Quantified population level responses from each microculture after 5 days of exposure to each of six signaling cues. Data were scaled and nondimensionalized using z-score method. Error bars represent a 95% confidence interval. (c) i. Marginal means analysis for main and pairwise interaction effects among all soluble cues for proliferative activity. FGF-2 and TGF-β interaction is highlighted with corresponding immunocytochemistry images of microcultures. Scale bar = 100 microns. ii. Marginal means interaction plots for glial response of FGF-2 in the presence of all other cues. iii. Marginal means plots for β-III-tubulin and neurite extensions of Wnt-3a and Ephrin-B2 with corresponding immunocytochemistry images of microcultures. Scale bar = 100 microns. Data were scaled and nondimensionalized using z-score method. Error bars represent a 95% confidence interval. BMP-4: bone morphogenetic protein 4; FGF-2: fibroblast growth factor 2; SHH-N: sonic hedgehog N-terminus; TGF- β: transforming growth factor β [Color figure can be viewed at wileyonlinelibrary.com]

additional measured variables using the appropriate positive and negative controls were calculated and are within range for an adequate screening assay (Zhang, Chung, & Oldenburg, 1999; Supporting Information Figure S3). Finally, we created a customized device to control the reproducibility of the micropillar transfer process between microwell chips (Supporting Information Video S1), an integral part of this microculture methodology. These data collectively demonstrate the ability to miniaturize NSC culture while maintaining rigorous quality control measures to enable high-throughput phenotypic screening of NSC proliferation and differentiation.

3.2 | Implementation of combinatorial signaling screen in the microchip system

We designated six endogenous signaling cues (FGF-2, SHH, Wnt-3a, Ephrin-B2, BMP-4, and TGF-β) from the adult hippocampal niche to be of particular interest for this combinatorial study because of their prominent roles in NSC regulation, their opposing effects on the NSC behavior as described above, and the lack of quantitative information on the potential interactions these cues may have with one another when simultaneously present in the niche. Therefore, a full factorial design of experiments methodology was used to explicitly quantify interaction effects between signaling cues (Box, Hunter, & Hunter, 2005; Figure 3ai). We first used a colorimetric dye to validate that our custom robotic liquid handling program was able to dispense all cues into the intended positions on the microwell chip to create 64 unique combinations from the six cues listed previously (Supporting Information Figure S4). Then, each cue was dispensed into the microwell chip at the EC_{50} dosage (Supporting Information Table S1). The complementary micropillar chip with NSCs was stamped into the microwell chip with media replenishment every other day. After 5 days in culture with combinatorial stimuli, quantitative population average measurements of multiple metrics were obtained, including the total cell count and the %EdU+ for a measure of proliferative activity, βIII-tubulin expression and neurite extension as a measure of neurogenicity, and GFAP expression as a measure of gliogenicity (Figure 3aii).

3.3 | Baseline activity of individual signals on NSC phenotype

To test the efficacy of each signaling cue to induce NSC response on-chip in accordance with previous literature, we examined the normalized endpoint phenotypes of NSC cultures exposed to each cue individually and compared them to the basal media condition of minimal FGF-2, which was chosen to maintain survival but not promote proliferation (Figure 3b). The basal media condition exhibited low levels of βIII-tubulin expression, likely due to spontaneous differentiation upon decreased FGF-2. Importantly, Wnt-3a or Ephrin-B2 increased βIII-tubulin expression consistent with reported literature (Ashton et al., 2012; Lie et al., 2005); FGF-2 induced proliferation (Palmer, 1995; Palmer et al., 1999); and TGF-β suppressed proliferation and differentiation of NSCs (Kandasamy et al., 2014; Yousef et al., 2015). Unexpectedly, we observed increased GFAP expression in response to

BMP-4, TGF-β, or Ephrin-B2 relative to the basal media condition. Finally, SHH showed increased but nonstatistical proliferative activity relative to the basal medium condition, potentially due to a less potent recombinant form of the molecule used here (Vazin et al., 2014). Overall, FGF-2, Wnt-3a, Ephrin-B2, and TGF-β induced NSC phenotypic responses in accordance with the literature, while BMP-4, TGF-β, and Ephrin-B2 were also found to increase GFAP expression—a trend not previously reported for adult hippocampal NSCs.

3.4 | Pairs of signaling cues exhibit additive, antagonistic, and synergistic relationships

Pairwise interactions were analyzed by examining how the extent of a specific NSC response induced by each signaling cue may be modulated by the presence of another potent signaling cue in the cellular microenvironment. A marginal means calculation was used to quantitatively discern the main effect of an individual cue from the interaction effect between two cues on the endpoint phenotypes measured (Box et al., 2005). Furthermore, the marginal means plots characterized the type of interaction between two signaling cues— Pairs of cues with parallel lines in the interaction plot were classified to have an additive relationship, while any deviation from parallel was classified as nonadditive (Box et al., 2005) and pointed to a pair of cues that act either antagonistically or synergistically to impact NSC proliferation or differentiation (Figure 3c and Supporting Information Figures S5, S6, and S7).

Many cues functioned additively, and thus did not point to statistical evidence of a potential biological interaction between the cues; however, nonadditive interactions occurred in several cases. The proliferative activity of FGF-2 on NSCs was found to be antagonistically modulated by the presence TGF-β or Wnt-3a (representative images of FGF-2 and TGF-β microcultures are depicted in Figure 3ci). TGF-β also affected the activity of Wnt-3a and Ephrin-B2 to decrease the extent of NSC proliferation. The most apparent trend for glial differentiation was the antagonistic activity of FGF-2 with all other cues, shown by a decrease of GFAP expression across all conditions with FGF-2 present. For neuronal differentiation, a single case of synergy was evident between Wnt-3a and Ephrin-B2 in the expression of βIII-tubulin and dendritic extensions. In summary, these data provide new information on how the activity of one endogenous cue may be modulated by the presence of just one additional signaling cue in the NSC microenvironment to impact NSC fate, and significantly narrows the field for interesting interactions to investigate further in vivo.

3.5 | Cooperative action by tertiary and quaternary signal combinations influences neuronal differentiation

Subsequently, we examined whether higher order combinations of signaling cues (e.g., interactions among three or more factors) in a microenvironment may interact uniquely to impact NSC behavior. We first used a factorial ANOVA to quantify the significance levels of all individual cues (main effect) and groups of cues (interaction effect)
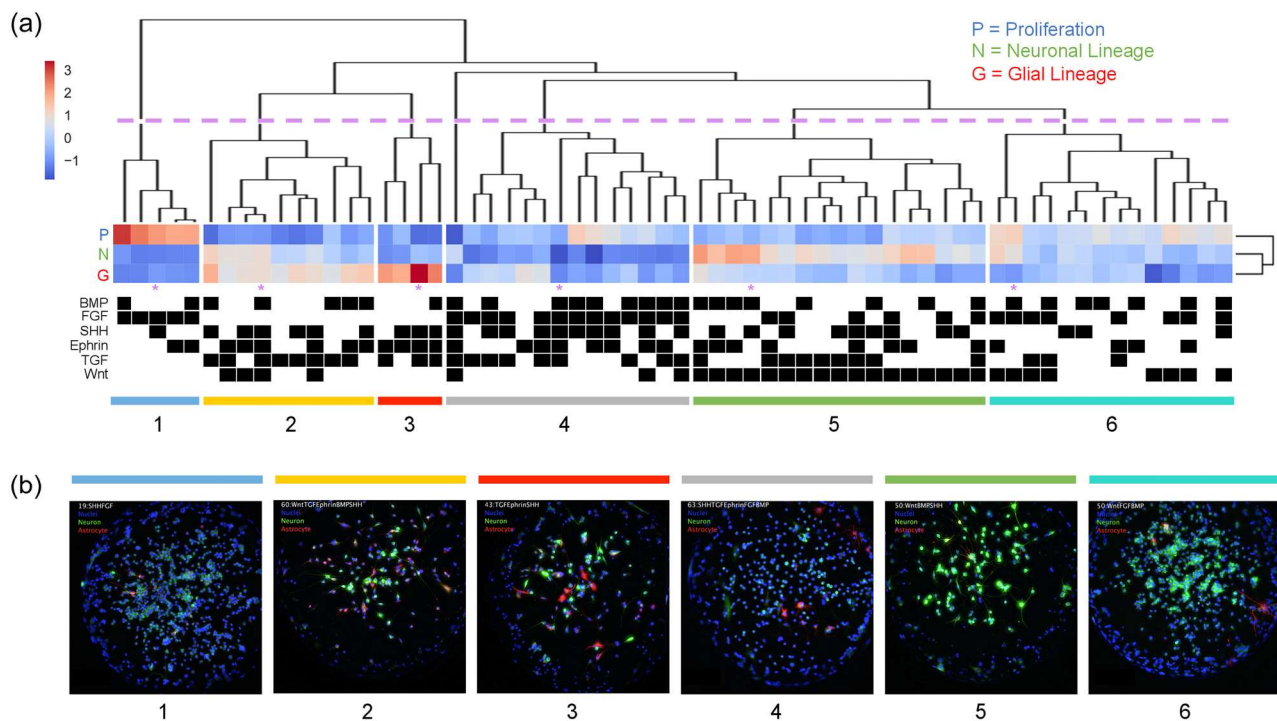
FIGURE 4 Factorial analysis of variance model for βIII-tubulin expression and neurite extensions. (a) *p* values of main and interaction effects for all signaling environments and the Benjamini and Hochberg threshold for multiple comparisons at a significance level of 0.05. (b) Pareto plot of fitted OLS model parameters for top 10 responses and corresponding immunocytochemistry images for the most positive (top) and most negative (bottom) contributions to βIII-tubulin expression and neurite extensions. Scale bar = 100 microns. BMP: bone morphogenetic protein; FDR: false discovery rate; FGF: fibroblast growth factor; OLS: ordinary least squares; SHH: sonic hedgehog; TGF: transforming growth factor [Color figure can be viewed at wileyonlinelibrary.com]

on NSC proliferation, glial differentiation, and/or neuronal differentiation, relative to the absence of that cue or group (Figure 4a and Supporting Information Figures S8 and S9) subject to a false-discovery rate correction (Benjamini & Hochberg, 1995). Then, we took the top 10 rank ordered combinations and created an OLS model to represent the relative impact of each signaling environment to the extent of proliferation or differentiation observed. One fourth-order combination was identified to have significant contributions to the extent of neurogenesis in a population, and specifically Wnt-3a + BMP-4 + Ephrin-B2 + TGF-β was found to drive neuronal differentiation to an extent greater than any of these components individually (Figure 4b). Interestingly, the main effect of Ephrin-B2 on βIII-tubulin expression and neurite extension was lesser in magnitude than the combined factors listed above (Figure 3ciii), yet

simply replacing Ephrin-B2 with SHH in the previous combination switched the outcome from a strong promotion to the strongest suppression of neurogenesis. These results point to a group of cues that act in a cooperative manner to impact the level of neurogenesis in adult NSCs. To examine if the microculture methodology might contain inherent confounding variables in this study, we conducted validation studies in an independent culture format (Supporting Information Figure S10).

3.6 | Global analysis of extrinsic signaling and phenotype relationship for NSC populations

To reveal additional trends within the multidimensional dataset, we described each signaling combination as a vector of the endpoint

FIGURE 5 Multivariate analysis of phenotypic response from combinatorial signaling environments. (a) Hierarchical cluster dendogram of main NSC phenotypes with corresponding signals present at each condition and six main classifications are identified by phenotype similarity; data are standardized by z-score for each measurement variable (row). (b) Corresponding immunocytochemistry images of microenvironments with asterisks in (a). BMP: bone morphogenetic protein; FGF: fibroblast growth factor; NSC: neural stem cell; SHH: sonic hedgehog; TGF: transforming growth factor [Color figure can be viewed at wileyonlinelibrary.com]

proliferation, neuronal differentiation, and glial differentiation and used a hierarchical clustering technique to arrange them into categories based on similarity in the direction and extent of the endpoint phenotypes observed (Figure 5).

The conditions with the most proliferation and least differentiation, marked as Category 1, all share the presence of FGF-2 and had a lower order combination of signals, that is, there was an average of only two signaling cues in the microenvironment. Category 4 also shared the presence of FGF-2 in most microenvironments, yet exhibited low proliferation and low differentiation. Ten out of the 13 conditions in Category 4 also had TGF-β and/or Wnt-3a present, which apparently antagonized the mitogenic activity of FGF-2 such that the combination showed very modest cell expansion. The remaining conditions in low proliferation and differentiation Category 4 contained combinations of BMP-4, SHH, and Ephrin-B2, where the average number of signaling cues per microenvironment was above three.

Two categories contained low proliferation and high differentiation responses into either neural or glial lineages, but not both. The most neurogenic category, Category 5, had conditions that all shared the presence of Wnt-3a. In contrast, the highest GFAP expressing category, marked as Category 3, had conditions that all shared the absence of FGF-2. Finally, the last two categories straddled the line between two phenotype directions: Category 2 contained low neural and low glial differentiation while Category 6 contained low proliferation and low neuronal differentiation. Interestingly, no categories were found that contained proliferation and glial differentiation together.

4 | DISCUSSION

4.1 | Combinatorial screening to accelerate understanding of the adult hippocampal NSC niche

Numerous insights have been gathered from miniaturization and high-throughput studies of stem cell niche components (Brafman et al., 2009; Rasi Ghaemi et al., 2016; Soen et al., 2006; Titmarsh et al., 2016). Here we provide a demonstration of the micropillar/microwell platform to expand beyond toxicology screening (Kwon et al., 2014; Lee et al., 2014; Nierode et al., 2016) and probe fundamental questions regarding how primary NSCs respond to combinatorial signals from the endogenous adult hippocampal niche. In doing so, we were able to simultaneously assay over 500 independent soluble microenvironments and acquire high-content images of NSC proliferation, differentiation, and morphological responses while consuming only 0.2% of the reagent volumes for conventional 96-well plates. Not only is this a favorable system for high-cost reagents, such as recombinant protein growth factors, but also for cell types that are difficult to expand. Furthermore, the parallel processing of 500 independent samples enabled a highly controlled and systematic study to probe phenotypic variations between signaling cue combinations while eliminating confounding variables such as cell passage number of primary NSCs, batch-to-batch variability and degradability of reagents, day-to-day variation in equipment parameters, or even person-to-person variations in

technique. We further discuss numerous results from the dataset below and provide a feasible parameter space for investigation in vivo.

4.2 | New phenotypes in response to BMP-4 and TGF-β signals

To our knowledge, this is the first report of BMP-4, TGF-β, or Ephrin-B2 signals increasing expression of GFAP in a population of adult hippocampal NSCs (Ashton et al., 2012; Bond et al., 2014; Conway et al., 2013; Mira et al., 2010; Yousef et al., 2014, 2015). In vivo, GFAP is expressed in Type 1 radial glial cells that are quiescent in the adult hippocampus as well as in lineage-committed astrocytes. Here, we observed two distinct morphologies of GFAP+ cells: One with multiple prominent extensions protruding from the cell body that resemble a characteristic example of an astrocyte, and the other with minor extensions from the cell body (Supporting Information Figure S2B). It is conceivable that the latter GFAP+ cell type is closer in identity to the Type 1 radial glial cell since BMP-4 and TGF-β are known to play a role in the regulation of quiescence of adult hippocampal NSCs (Figure 3ci). To further investigate a potential role for BMP-4 or TGF-β as a cue to revert Type 2 neural progenitor towards Type 1 radial glial cells, future work could examine the effect of BMP-4 or TGF-β exposure on the population of Type 1 radial glial cells, identified by coexpression of GFAP and NSC markers such as Nestin or Sox2.

4.3 | Convergence to an outcome by the integration of simultaneous signals

At the signal transduction level, the numerous extrinsic signaling molecules, and combinations thereof, that exist within the stem cell niche to influence cell fate are ultimately translated to relatively few phenotypes, pointing to the existence of integration mechanisms within the cell that converge inputs to reach an outcome. For adult hippocampal NSCs, this concept has been discussed previously by Schwarz, Ebert, and Lie (2012) with Notch signaling proposed as a central node of convergence for BMP-4, TGF-β, SHH, and FGF-2 signals. Here, we uncover additional interactions involving cues discussed by Schwarz et al. as well as Wnt-3a and Ephrin-B2 that influence the phenotypic outcome of NSCs. The molecular basis of these interactions is likely unique for each pair or combination and could assume multiple forms including an extracellular interaction between ligands, such as the mechanism described for the antagonistic relationship between Noggin and BMP signaling cues (Lim et al., 2000). Additional hypotheses for intracellular mechanisms could include signal pathway crosstalk at the level of phosphorylation cascade or transcription factor, or priming by translocation of key intermediates by one pathway for the other.

The unique case of synergy we observed between Wnt-3a and Ephrin-B2 to increase β-III-tubulin expression and neurite extensions is of particular interest to investigate further. Previous studies showed that Ephrin-B2 can activate the coactivator β-catenin, pointing to a possible node of convergence between the two pathways (Ashton et al., 2012). Additionally, a link between the

Ephrin and Wnt signaling pathways has been established in the analogous adult stem cell system of the intestinal crypt, where canonical Wnt signaling through β-catenin was found to upregulate the expression of EphB2/EphB3 receptors (Batlle et al., 2002). Given that many aspects of signal transduction are conserved across various cell types, it is conceivable that a similar signaling network layout is present here in adult hippocampal NSCs.

The majority of higher order combinations of signals probed in other differentiated cell types have exhibited negligible synergy at the level of intracellular signaling cascades, as reviewed previously by Janes and Lauffenburger (2013). Our results from the factorial ANOVA and OLS modeling indicate that this paradigm can potentially be extended to NSC population level responses to combinatorial stimuli as well (Figure 4 and Supporting Information Figures S7 and S8). However, as described in the next section, even a single case of higher order combinatorial interactions can provide a fruitful area of further investigation to understand combinatorial complexity in stem cell niches, and therefore including them in systematic screening efforts early on might be worthwhile for stem cell differentiation in particular, as their developmental outcome might by more flexible and sensitive to higher order combinations of signals than terminally differentiated cell types.

4.4 | Niche zones that display the clearest "instructions" for a specific phenotypic response

At the niche level, it is conceivable that there is heterogeneity in signal presentation across local NSC microenvironments that contributes to the range of fate outcomes for NSCs within the dentate gyrus (Bonaguidi et al., 2011; Pilz et al., 2018). The results in this study point to details of extrinsic signaling combinations that might shift NSC fate outcome toward proliferation, quiescence, or differentiation.

The most proliferative NSC response in microenvironments occurred with FGF-2 alone. The presence of additional cues either had negligible effect (BMP-4) or acted antagonistically (Ephrin-B2, TGF-β, and Wnt-3a). Therefore, it is possible that NSCs undergoing the most proliferation and potentially self-renewal are located in zones of FGF-2 exposure, with minimum conflicting signals. In contrast, there is a shift toward quiescence in zones that present numerous conflicting signals, such as FGF-2, Wnt-3a, and TGF-β together. Additionally, these observations point to a dual role for FGF-2 as mainly proliferative in simple (i.e., one or two cues) signaling environments, and mainly repressive of differentiation in more complex signaling environments.

The higher order combination of Wnt-3a + Ephrin-B2 + BMP-4 + TGF-β could provide a neurogenic and neuronal maturation niche. The contrasting role of TGF-β in this combination versus in isolation is noteworthy. Previous reports have provided evidence for dual roles of BMP-4 and TGF-β as quiescence factors for NSCs and maturation factors for committed neuroblasts (He et al., 2014; Kandasamy et al., 2014), which could explain the results observed here. It is conceivable that the initial exposure of NSCs to Wnt-3a + Ephrin-B2 to induce

neuroblast commitment while the simultaneous presence of Wnt-3a + Ephrin-B2 with BMP-4 + TGF-β in a niche could induce neuroblast commitment and accelerate the maturation process. In vivo, migration of neuroblasts away from the subgranular zone during maturation may alternatively offer a mechanism where the presence of BMP-4 + TGF-β is in a spatially distinct zone, to enable sequential exposure to different signals as cells progress down a neuronal lineage. Either way, the signals appear to cooperate to influence neuronal differentiation and maturation.

4.5 | Context dependence of NSC fate

Overall, the various cases of signaling interactions identified here and their implications in NSC signal transduction and for the NSC niche share a larger theme of context dependence, where the activity of multiple signaling cues is modulated by the presence of additional cues in the microenvironment of an NSC. These studies quantitatively demonstrate that a highly intricate and sensitive balance of multiple cues guides the endpoint phenotype of NSC populations and these in vitro results are potentially representative of NSC fate within the adult hippocampal niche. Disruption of precise balances between molecular cues could contribute to the cell and tissue degeneration in the hippocampus during aging (Mosher & Schaffer, 2018) or by disease, having consequences for learning and memory throughout adulthood.

5 | CONCLUSION

The novel application of a high-throughput micropillar/microwell methodology enabled careful and systematic dissection of the combinatorial signaling niche. Interactions between key endogenous cues can play a large role in the regulation of NSC phenotypes, and the quantitative analyses presented here identify numerous cases of signaling context dependence. These data also provide promising leads for an in vivo investigation of the implications of combinatorial signals, such as the antagonism between FGF-2 and TGF-β, or the synergistic neurogenesis from Wnt-3a + Ephrin-B2 + BMP-4 + TGF-β. Overall, this study contributes to further understanding of the intricate and complex mechanisms guiding NSC fate choice, and provides insight that may enhance control over stem cell-based therapies for neurodegenerative diseases.

CONFLICTS OF INTEREST

The authors declare that there are no conflicts of interest.

AUTHOR CONTRIBUTIONS

D. S. C. and D. V. S. conceived the project and supervised the studies. S. K. M, B. C. P., and R. M. set up experimental systems. R. M. designed experiments and managed workflows. C. Y. synthesized multivalent Ephrin. R. M., M. G., A. M., and E. T. executed experimental and computational workflows. R. M., C. Y., D. S. C., and D. V. S. analyzed and interpreted data. R. M. wrote the manuscript with revisions from D. S. C., D. V. S. and J. S. D.

ORCID

Jonathan S. Dordick 🔴 http://orcid.org/0000-0001-7802-3702
David V. Schaffer 🔴 http://orcid.org/0000-0002-9625-0121

REFERENCES

Ashton, R. S., Conway, A., Pangarkar, C., Bergen, J., Lim, K.-I., Shah, P., … Schaffer, D. V. (2012). Astrocytes regulate adult hippocampal neurogenesis through ephrin-B signaling. *Nature Neuroscience*, *15*(10), 1399–1406. https://doi.org/10.1038/nn.3212

Avior, Y., Sagi, I., & Benvenisty, N. (2016). Pluripotent stem cells in disease modelling and drug discovery. *Nature Reviews Molecular Cell Biology*, *17*(3), 170–182. https://doi.org/10.1038/nrm.2015.27

Bankhead, P. (2014). Analyzing fluorescence microscopy images with ImageJ. *ImageJ*, *1*, 1–195. https://doi.org/10.1109/NER.2015.7146654

Batlle, E., Henderson, J. T., Beghtel, H., van den Born, M. M. W., Sancho, E., Huls, G., … Clevers, H. (2002). Beta-catenin and TCF mediate cell positioning in the intestinal epithelium by controlling the expression of EphB/ephrinB. *Cell*, *111*(2), 251–263. https://doi.org/10.1016/S0092-8674(02)01015-2

Benjamini, Y., & Hochberg, Y. (1995). Controlling the false discovery rate: A practical and powerful approach to multiple testing. *Journal of the Royal Statistical Society. Series B (Methodological)*, *57*, 289–300. https://doi.org/10.2307/2346101

Bonaguidi, M. A., Wheeler, M. A., Shapiro, J. S., Stadel, R. P., Sun, G. J., Ming, G., & Song, H. (2011). In vivo clonal analysis reveals self-renewing and multipotent adult neural stem cell characteristics. *Cell*, *145*(7), 1142–1155. https://doi.org/10.1016/J.CELL.2011.05.024

Bond, A. M., Peng, C. Y., Meyers, E. A., McGuire, T., Ewaleifoh, O., & Kessler, J. A. (2014). BMP signaling regulates the tempo of adult hippocampal progenitor maturation at multiple stages of the lineage. *Stem Cells*, *32*(8), 2201–2214. https://doi.org/10.1002/stem.1688

Boutros, M., Heigwer, F., & Laufer, C. (2015). Microscopy-based high-content screening. *Cell*, *163*(6), 1314–1325. https://doi.org/10.1016/j.cell.2015.11.007

Box, G. E. P., Hunter, W. G., & Hunter, J. S. (2005). *Statistics for experimenters*. John Wiley & Sons, Inc.

Brafman, D. A., de Minicis, S., Seki, E., Shah, K. D., Teng, D., Brenner, D., … Chien, S. (2009). Investigating the role of the extracellular environ-

ment in modulating hepatic stellate cell biology with arrayed combinatorial microenvironments. *Integrative Biology: Quantitative Biosciences from Nano to Macro*, *1*(8–9), 513–524. https://doi.org/10.1039/b912926j

Conway, A., Vazin, T., Spelke, D. P., Rode, N. A., Healy, K. E., Kane, R. S., & Schaffer, D. V. (2013). Multivalent ligands control stem cell behaviour in vitro and in vivo. *Nature Nanotechnology*, *8*(11), 831–838. https://doi.org/10.1038/nnano.2013.205

Flaim, C. J., Teng, D., Chien, S., & Bhatia, S. N. (2008). Combinatorial signaling microenvironments for studying stem cell fate. *Stem Cells and Development*, *17*(1), 29–39. https://doi.org/10.1089/scd.2007.0085

Gage, F. H., Kempermann, G., Palmer, T. D., Peterson, D. A., & Ray, J. (1998). Multipotent progenitor cells in the adult dentate gyrus. *Journal of Neurobiology*, *36*(2), 249–266. http://www.ncbi.nlm.nih.gov/pubmed/9712308

Gobaa, S., Hoehnel, S., Roccio, M., Negro, A., Kobel, S., & Lutolf, M. P. (2011). Artificial niche microarrays for probing single stem cell fate in high throughput. *Nature Methods*, *8*(11), 949–955. https://doi.org/10.1038/nmeth.1732

Gonçalves, J. T., Schafer, S. T., & Gage, F. H. (2016). Adult neurogenesis in the hippocampus: From stem cells to behavior. *Cell*, *167*, 897–914. https://doi.org/10.1016/j.cell.2016.10.021

He, Y., Zhang, H., Yung, A., Villeda, S. A., Jaeger, P. A., Olayiwola, O., ... Wyss-Coray, T. (2014). ALK5-dependent TGF-β 2 signaling is a major determinant of late-stage adult neurogenesis. *Nature Neuroscience*, *17*(7), 943–952. https://doi.org/10.1038/nn.3732

Janes, K. A., & Lauffenburger, D. A. (2013). Models of signalling networks—What cell biologists can gain from them and give to them. *Journal of Cell Science*, *126*(Pt 9), 1913–1921. https://doi.org/10.1242/jcs.112045

Kandasamy, M., Lehner, B., Kraus, S., Sander, P. R., Marschallinger, J., Rivera, F. J., ... Aigner, L. (2014). TGF-beta signalling in the adult neurogenic niche promotes stem cell quiescence as well as generation of new neurons. *Journal of Cellular and Molecular Medicine*, *18*(7), 1444–1459. https://doi.org/10.1111/jcmm.12298

Koolpe, M., Burgess, R., Dail, M., & Pasquale, E. B. (2005). EphB receptor-binding peptides identified by phage display enable design of an antagonist with ephrin-like affinity. *Journal of Biological Chemistry*, *280*(17), 17301–17311. https://doi.org/10.1074/jbc.M500363200

Kwon, S. J., Lee, D. W., Shah, D. A., Ku, B., Jeon, S. Y., Solanki, K., ... Lee, M. Y. (2014). High-throughput and combinatorial gene expression on a chip for metabolism-induced toxicology screening. *Nature Communications*, *5*, 3739. https://doi.org/10.1038/ncomms4739

LaBarge, M. A., Nelson, C. M., Villadsen, R., Fridriksdottir, A., Ruth, J. R., Stampfer, M. R., ... Bissell, M. J. (2009). Human mammary progenitor cell fate decisions are products of interactions with combinatorial microenvironments. *Integrative Biology: Quantitative Biosciences from Nano to Macro*, *1*(1), 70–79. https://doi.org/10.1039/b816472j

Lader, J., Stachel, M., & Bu, L. (2017). Cardiac stem cells for myocardial regeneration: Promising but not ready for prime time. *Current Opinion in Biotechnology*, *47*, 30–35. https://doi.org/10.1016/j.copbio.2017.05.009

Lai, K., Kaspar, B. K., Gage, F. H., & Schaffer, D. V. (2003). Sonic hedgehog regulates adult neural progenitor proliferation in vitro and in vivo. *Nature Neuroscience*, *6*(1), 21–27. https://doi.org/10.1038/nn983

Lai, K., Robertson, M. J., & Schaffer, D. V. (2004). The sonic hedgehog signaling system as a bistable genetic switch. *Biophysical Journal*, *86*(5), 2748–2757. https://doi.org/10.1016/S0006-3495(04)74328-3

Lee, D. W., Choi, Y.-S., Seo, Y. J., Lee, M.-Y., Jeon, S. Y., Ku, B., ... Nam, D. H. (2014). High-throughput screening (HTS) of anticancer drug efficacy on a micropillar/microwell chip platform. *Analytical Chemistry*, *86*(1), 535–542. https://doi.org/10.1021/ac402546b

Lein, E. S., Hawrylycz, M. J., Ao, N., Ayres, M., Bensinger, A., Bernard, A., ... Jones, A. R. (2007). Genome-wide atlas of gene expression in the adult mouse brain. *Nature*, *445*(7124), 168–176. https://doi.org/10.1038/nature05453

Lie, D.-C., Colamarino, S. A., Song, H.-J., Désiré, L., Mira, H., Consiglio, A., ... Gage, F. H. (2005). Wnt signalling regulates adult hippocampal neurogenesis. *Nature*, *437*(7063), 1370–1375. https://doi.org/10.1038/nature04108

Lim, D. A., Tramontin, A. D., Trevejo, J. M., Herrera, D. G., García-Verdugo, J. M., & Alvarez-Buylla, A. (2000). Noggin antagonizes BMP signaling to create a niche for adult neurogenesis. *Neuron*, *28*(3), 713–726. https://doi.org/10.1016/S0896-6273(00)00148-3

Malo, N., Hanley, J. A., Cerquozzi, S., Pelletier, J., & Nadon, R. (2006). Statistical practice in high-throughput screening data analysis. *Nature Biotechnology*, *24*(2), 167–175. https://doi.org/10.1038/nbt1186

Mira, H., Andreu, Z., Suh, H., Lie, D. C., Jessberger, S., Consiglio, A., ... Gage, F. H. (2010). Signaling through BMPR-IA regulates quiescence and long-term activity of neural stem cells in the adult hippocampus. *Cell Stem Cell*, *7*(1), 78–89. https://doi.org/10.1016/J.STEM.2010.04.016

Mosher, K. I., & Schaffer, D. V. (2018). Influence of hippocampal niche signals on neural stem cell functions during aging. *Cell and Tissue Research*, *371*(1), 115–124. https://doi.org/10.1007/s00441-017-2709-6

Nierode, G. J., Perea, B. C., McFarland, S. K., Pascoal, J. F., Clark, D. S., Schaffer, D. V., & Dordick, J. S. (2016). High-throughput toxicity and phenotypic screening of 3d human neural progenitor cell cultures on a microarray chip platform. *Stem Cell Reports*, *7*(5), 970–982. https://doi.org/10.1016/j.stemcr.2016.10.001

Palmer, T. D. (1995). FGF-2-responsive neuronal progenitors reside in proliferative and quiescent regions of the adult rodent brain. *Molecular and Cellular Neuroscience*, *6*(5), 474–486. https://doi.org/10.1006/mcne.1995.1035

Palmer, T. D., Markakis, E. A., Willhoite, A. R., Safar, F., & Gage, F. H. (1999). Fibroblast growth factor-2 activates a latent neurogenic program in neural stem cells from diverse regions of the adult CNS. *The Journal of Neuroscience*, *19*(19), 8487–8497. http://www.ncbi.nlm.nih.gov/pubmed/10493749

Peltier, J., Agrawal, S., Robertson, M. J., Schaffer, D. V., Conboy, I. M., & Li, S. (2010). Protocols for adult stem cells. *Methods in Molecular Biology*, *621*, 203. https://doi.org/10.1007/978-1-60761-063-2

Pelttari, K., Mumme, M., Barbero, A., & Martin, I. (2017). Nasal chondrocytes as a neural crest-derived cell source for regenerative medicine. *Current Opinion in Biotechnology*, *47*, 1–6. https://doi.org/10.1016/j.copbio.2017.05.007

Pilz, G.-A., Bottes, S., Betizeau, M., Jörg, D. J., Carta, S., Simons, B. D., ... Jessberger, S. (2018). Live imaging of neurogenesis in the adult mouse hippocampus. *Science*, *359*(6376), 658–662. https://doi.org/10.1126/science.aao5056

Pool, M., Thiemann, J., Bar-Or, A., & Fournier, A. E. (2008). NeuriteTracer: A novel ImageJ plugin for automated quantification of neurite outgrowth. *Journal of Neuroscience Methods*, *168*, 134–139. https://doi.org/10.1016/j.jneumeth.2007.08.029

Rasi Ghaemi, S., Delalat, B., Cetó, X., Harding, F. J., Tuke, J., & Voelcker, N. H. (2016). Synergistic influence of collagen I and BMP 2 drives osteogenic differentiation of mesenchymal stem cells: A cell microarray analysis. *Acta Biomaterialia*, *34*, 41–52. https://doi.org/10.1016/j.actbio.2015.07.027

Roccio, M., Gobaa, S., Lutolf, M. P., Suh, H., Deng, W., Gage, F. H., & Brown, P. O. (2012). High-throughput clonal analysis of neural stem cells in microarrayed artificial niches. *Integrative Biology: Quantitative Biosciences from Nano to Macro*, *4*(4), 391–400. https://doi.org/10.1039/c2ib00070a

Rodrigues, M. T., Gomes, M. E., & Reis, R. L. (2011). Current strategies for osteochondral regeneration: From stem cells to pre-clinical approaches. *Current Opinion in Biotechnology*, *22*, 726–733. https://doi.org/10.1016/j.copbio.2011.04.006

Rossi, S. L., & Keirstead, H. S. (2009). Stem cells and spinal cord regeneration. *Current Opinion in Biotechnology*, *20*, 552–562. https://doi.org/10.1016/j.copbio.2009.09.008

Schwarz, T. J., Ebert, B., & Lie, D. C. (2012). Stem cell maintenance in the adult mammalian hippocampus: A matter of signal integration? *Developmental Neurobiology*, *72*(7), 1006–1015. https://doi.org/10.1002/dneu.22026

Soen, Y., Mori, A., Palmer, T. D., & Brown, P. O. (2006). Exploring the regulation of human neural precursor cell differentiation using arrays of signaling microenvironments. *Molecular Systems Biology*, *2*, 37. https://doi.org/10.1038/msb4100076

Titmarsh, D. M., Glass, N. R., Mills, R. J., Hidalgo, A., Wolvetang, E. J., Porrello, E. R., ... Cooper-White, J. J. (2016). Induction of human iPSC-derived cardiomyocyte proliferation revealed by combinatorial screening in high density microbioreactor arrays. *Scientific Reports*, *6*, 24637. https://doi.org/10.1038/srep24637

Vazin, T., Ashton, R. S., Conway, A., Rode, N. A., Lee, S. M., Bravo, V., ... Schaffer, D. V. (2014). The effect of multivalent sonic hedgehog on differentiation of human embryonic stem cells into dopaminergic and GABAergic neurons. *Biomaterials*, *35*(3), 941–948. https://doi.org/10.1016/j.biomaterials.2013.10.025

Wang, Z., Calpe, B., Zerdani, J., Lee, Y., Oh, J., Bae, H., ... Kim, K. (2016). High-throughput investigation of endothelial-to-mesenchymal transformation (EndMT) with combinatorial cellular microarrays. *Biotechnology and Bioengineering*, *113*(7), 1403–1412. https://doi.org/10.1002/bit.25905

Yousef, H., Conboy, M. J., Morgenthaler, A., Schlesinger, C., Bugaj, L., Paliwal, P., ... Schaffer, D. (2015). Systemic attenuation of the TGF-β pathway by a single drug simultaneously rejuvenates hippocampal neurogenesis and myogenesis in the same old mammal. *Oncotarget*, *6*(14), 11959–11978. http://www.impactjournals.com/oncotarget/index.php?journal=oncotarget&page=article&op=view&path%5B%5D=3851&path%5B%5D=8731

Yousef, H., Morgenthaler, A., Schlesinger, C., Bugaj, L., Conboy, I. M., & Schaffer, D. V. (2014). Age-associated increase in BMP signaling inhibits hippocampal neurogenesis. *Stem Cells*, *33*(5), 1577–1588. https://doi.org/10.1002/stem.1943

Zhang, J. H., Chung , T. D., & Oldenburg, K. R. (1999). A simple statistical parameter for use in evaluation and validation of high throughput screening assays. *Journal of Biomolecular Screening*, *4*(2), 67–73. http://www.ncbi.nlm.nih.gov/pubmed/10838414

SUPPORTING INFORMATION

Additional supporting information may be found online in the Supporting Information section at the end of the article.